Effect of Pressure on Proton Transfer Rate from a Photoacid to a Solvent. 3. 2-Naphthol and 2-Naphthol Monosulfonate Derivatives in Water

Liat Genosar, Pavel Leiderman, Nahum Koifman, and Dan Huppert*

Raymond and Beverly Sackler Faculty of Exact Sciences, School of Chemistry, Tel Aviv University, Tel Aviv 69978, Israel

Received: September 23, 2003; In Final Form: January 8, 2004

The reversible proton dissociation and geminate recombination of three photoacids, 2-naphthol, 2-naphthol-7-sulfonate, and 2-naphthol-8-sulfonate, are studied at various pressures in water. The results are compared with the results of the pressure dependence study we recently conducted for 2-naphthol-6-sulfonate in water and 5,8-dicyanonaphthol in ethanol and propanol. Our time-resolved experimental data are analyzed by the reversible diffusion-influenced chemical reaction model. The proton transfer rate increases significantly with pressure: at ∼11 kbar, the rate increases by a factor in the range of 7.5−10. The pressure dependence is explained using an approximate stepwise two coordinate proton-transfer model. The model is compared with the Landau−Zener curve-crossing proton tunneling formulation. The increase in rate, as a function of pressure, manifests, on one hand, the strong dependence of proton tunneling on the distance between the two oxygen atoms involved in the process, which decreases with an increase of pressure, and, on the other hand, the small change in the water relaxation rate as a function of pressure.

Introduction

Proton transfer to a solvent (PTTS) is a fundamental process in chemistry and biology.[1,2] In solution, it determines acid−base reactivity and is connected to factors governing proton association, solvation and mobility. The phenomenon of excited-state proton transfer (ESPT) from a photoacid molecule that dissociates upon excitation to produce an excited anion and a proton[3−6] was used in time-resolved studies of proton-transfer reactions in liquids and solids. Recent studies[7−14] emphasize the dual role played by the solvent molecule (1) as a proton acceptor and (2) as a solvating medium of both the reactant and the product.[15−17]

Theoretical studies revealed that tunneling is the dominant reaction mode for proton transfer, even at ambient temperatures. The theory of the proton-transfer reaction in solution was developed by Dogonadze, Kuznetzov, Ulstrup, and co-workers[18,19] and then extended by Borgis and Hynes,[20] Kiefer and Hynes,[21] Cukier,[22] Voth,[23] and Hammes-Schiffer.[24] These theories show that the presence of a potential energy barrier in the proton-reaction coordinate causes tunneling through the barrier in the reaction pathway, as opposed to passage over the barrier.

Ando and Hynes[25] studied the acid ionization of HCl in water via a combination of electronic structure calculations and Monte Carlo computer simulations. The mechanism is found to involve first, an activationless (or nearly so) motion in a solvent coordinate, which is adiabatically followed by the quantum proton, to produce a "contact" ion pair Cl^- H_3O^+, which is stabilized by ∼ 7 kcal/mol, and second, motion in the solvent with a small activation barrier, as a second adiabatic proton transfer produces a "solvent-separated" ion pair from the "contact" ion pair in a nearly thermoneutral process.[25]

Pressure is known to influence the rate of chemical reactions in the condensed phase. External pressure changes such properties of the medium and reactants as the reaction free volume, potential energy profile along the reaction path, compressibility, viscosity, and the reorganization energy of the medium.[26] The absolute value of the reaction rate constant and its temperature dependence can depend on all of these parameters. The pressure influences both the characteristics of classical over-barrier reactions and the tunneling transfer of the proton. The pressure influence on tunneling in the solid state is discussed in refs 26 and 27. In solids, the tunneling reaction depends exponentially on both the equilibrium distance between the reactants and the frequency of intermolecular vibrations, which varies with compression.

In previous papers,[10−13] we described our experimental results of an unusual temperature dependence of the excited-state proton transfer from a photoacid to liquid water, monols, diols, and glycerol. In methanol and ethanol at temperatures above 285 K, the rate of the proton transfer is almost temperature independent while, at $T < 250$ K, the rate exhibits great temperature dependence. The rate constant is similar to the inverse of the longest component of the dielectric relaxation time of a particular protic solvent.

We proposed a simple stepwise model to describe and calculate the temperature dependence of the proton transfer to the solvent reaction. The model accounts for the large difference in the temperature dependence, the proton-transfer rate at high and low temperatures, and the solvent dependencies. The proton-transfer reaction depends on two coordinates, the first of which depends on the generalized solvent configuration. The solvent coordinate characteristic time is within the range of the dielectric relaxation time, τ_D, and the longitudinal relaxation, $\tau_L = (\epsilon_\infty/\epsilon_0)\tau_D$, where ϵ_0 and ϵ_∞ are the static and high-frequency dielectric constants, respectively. The second coordinate is the actual proton translational motion (tunneling) along the reaction

* To whom correspondence should be addressed. E-mail: huppert@tulip.tau.ac.il. Fax/Phone: 972-3-6407012.

10.1021/jp0310910 CCC: $27.50
Published on Web 02/14/2004

path. The model restricts the proton transfer process to a stepwise one. The proton moves to the adjacent hydrogen bonded solvent molecule only when the solvent configuration brings the system to the crossing point.

The unusual temperature dependence of the proton-transfer rate is explained as follows: the high-temperature behavior of the proton-transfer rate constant is controlled by the proton tunneling rate, whereas at low temperature, the solvent motion controls the rate. We used an approximate expression for the proton-transfer rate, which bridges the high-temperature proton tunneling limit and the solvent controlled limit to fit the temperature dependence curve of the experimental proton-transfer rate constant at all temperatures, see eq 4.

In recent studies,[28,29] we measured, using time-resolved emission techniques, the proton dissociation from a strong photoacid, 5,8 -dicyano-2-naphthol (DCN2) as a function of pressure in both ethanol and propanol. In ethanol, we found that the proton dissociation rate constant, k_{PT}, of excited DCN2 at relatively low pressures (up to 10 kbar) increases with pressure. At about 10 kbar, it reaches the largest rate, about twice the rate at atmospheric pressure. At higher pressures, up to the freezing point of ethanol, about 1.9 GPa, the proton-transfer rate decreases with pressure and its value in the high-pressure regime is similar to the inverse of the dielectric relaxation time.

We applied the stepwise two coordinate model that was successfully used to fit the temperature dependence of the proton transfer rate to also fit the pressure dependence. For the ethanol solution, analysis of the experimental data showed that pressure affects both the solvent and the proton coordinates, but in opposite directions. The proton tunneling rate increases with pressure, whereas the solvent relaxation in ethanol decreases significantly with pressure.

For propanol, we found that the proton dissociation rate constant, k_{PT}, of excited DCN2 at relatively low pressures (up to 5 kbar) increases slightly with pressure. At 5 kbar, the rate is 20% larger than the value at atmospheric pressure, whereas at higher pressures up to ~2.5 GPa (25 kbar), the proton-transfer rate decreases with pressure and its value is related to the inverse of the dielectric relaxation time. At about 2.2 GPa, the rate is smaller by a factor of about 20 than that at atmospheric pressure. The increase in the proton tunneling rate at low pressures, increases the overall rate, k_{PT}, slightly. The solvent coordinate rate strongly affects k_{PT} at high pressures. At a pressure above 5 kbar, k_{PT} is mainly determined by the solvent coordinate rate, i.e., the solvent controlled limit.

In contrast to DCN2−propanol, we found in a recent study of proton transfer from 2-naphthol-6-sulfonate to water[30] that pressure only mildly affects the solvent coordinate rate of water, whereas the tunneling rate increases almost 10-fold with pressure. The overall effect is a strong increase of the proton-transfer rate, k_{PT}, with pressure.

In this paper, we further explore the effect of pressure on excited-state intermolecular proton transfer (ESPT) dynamics in water. For this purpose, we chose four photoacids: 2-naphthol (2N), 2-naphthol-7-sulfonate (2N7S), 2-naphthol-8-sulfonate (2N8S), and 8-hydroxy-1,3,6-pyrenetrisulfonate (HPTS). Fox and co-workers studied the proton-transfer rate in supercritical water.[31] They used pressures up to 300 atm at elevated temperatures, up to 200 °C. As the temperature increases, the rate decreases. The decrease in the proton-transfer rate at high temperatures is due to breaking the water structure, which is manifested by a low dielectric constant of water at 200 °C, $\epsilon \approx 35$. In the past, we studied the pressure dependence of the proton-transfer rate from HPTS to water.[32] The rate increases mildly with pressure. In this previous study[32] we used a streak camera to time-resolve the luminescence with a relatively small S/N ratio. In addition, we did not use the reversible geminate proton recombination model in the luminescence data analysis. We therefore decided to remeasure the pressure dependence of the proton-transfer rate from HPTS to water. For all these photoacids, we found an increase of the proton-transfer rate as a function of pressure by a factor of between 3 (for HPTS, where the rates values are the highest) and 9 (for 2N7S). We used our qualitative stepwise two coordinate model to explain the strong pressure effect on proton transfer. The model can be related to theories of proton transfer,[20,18] based on the Landau−Zener curve crossing formulation.

Experimental Section

Pressurized time-resolved emission was measured in a compact gasketed diamond anvil cell[33] (DAC) purchased from D'Anvil[34,35] with 0.3 carat low fluorescent high UV transmission diamonds.

To provide a larger volume of the sample for sufficient fluorescent intensity, a 0.45 mm hole was drilled in the 0.8 mm thick stainless gasket. The low fluorescence-type diamonds served as anvils. The anvil seats were with suitable circular apertures for the entry and exit of the exciting laser beam and the excited fluorescent intensity. With this cell, pressures up to 30 kbar were reached, without detriment to the diamond anvils. The pressure generated was calibrated using the well-known ruby fluorescent technique.[36]

Time-resolved fluorescence was measured using the time-correlated single-photon counting (TCSPC) technique. As an excitation source, we used a cw mode-locked Nd:YAG-pumped dye laser (Coherent Nd:YAG Antares and a 702 dye laser), providing a high repetition rate (>1 MHz) of short pulses (2 ps at full width half-maximum, fwhm). The (TCSPC) detection system is based on a Hamamatsu 3809U, photomultiplier, Tennelec 864 TAC, Tennelec 454 discriminator and a personal computer-based multichannel analyzer (nucleus PCA-II). The overall instrumental response was about 50 ps (fwhm). Measurements were taken at 10 nm spectral width.

2-Naphthol, 2-naphthol-6-sulfonate, and HPTS were purchased from Kodak. 2-Naphthol-7-sulfonate and 2-naphthol-8-sulfonate were purchased from TCI. All compounds were used without further purification. The sample concentrations were between 1×10^{-3} and 3×10^{-4} M using deionized water of 10 MΩ resistance. The solution's pH was approximately 6.

The fluorescence spectrum belonging to 2-naphthol, 2-naphthol-7-sulfonate, 2-naphthol-8-sulfonate, and HPTS consists of two structureless broad bands (~40 nm fwhm). The emission band maximum of the acidic form (ROH*) of the naphthol and naphthol sulfonate derivatives in water and alcohols emits at about 350 nm. The emission band maximum of the alkaline form (RO^-*) in water and alcohols emits at about 420 nm. At 350 nm, the overlap of the two-luminescence bands is rather small and the contribution of the RO^-* band to the total intensity at 350 nm is less than 1%. At 1 atm, the impurity and dimer emission level is about 0.2% of the peak intensity at 350 nm and increases up to 1% at 10 kbar. Therefore, in the analysis of the time-resolved emission data, we add to the calculated signal an additional component with an exponential decay of about 10 ns, with amplitude of about 0.2% at 1 atm, which increases with pressure up to 1% at 10 kbar to account for the impurity fluorescence. To avoid ambiguity, due to the overlap between

SCHEME 1

$$ROH^* \underset{k_r}{\overset{k_{PT}}{\rightleftharpoons}} [RO^-{}^* \ldots H^+]_{(r=a)} \overset{DSE}{\rightleftharpoons} RO^-{}^* + H^+$$

the fluorescence contributions of ROH* and RO^-*, and in order to minimize the impurity fluorescence, we mainly monitored the ROH* fluorescence at 350 nm. For HPTS, ROH*, and RO^-*, bands are located at 440 and 510 nm respectively.

Results

Reversible Diffusion Influenced Two Step Model. Previous studies of reversible ESPT processes in solution led to the development of a reversible diffusion influenced two step model[37,38] (Scheme 1).

In the continuous diffusion approach, the photoacid dissociation reaction is described by the spherically symmetric diffusion equation (DSE)[39] in three dimensions.[37,38] The boundary conditions at $r = a$ are those of the back reaction (Scheme 1). k_{PT} and k_r are the "intrinsic" dissociation and recombination rate constants at the contact sphere radius, a. Quantitative agreement was obtained between the model and the experiment.[37,38] A detailed description of the model, as well as the fitting procedure, is given in refs 9, 37, and 38.

Comparison of the numerical solution with the experimental results involves several parameters. Usually, the adjustable parameters are the proton-transfer rate to the solvent, k_{PT}, and the geminate recombination rate, k_r. The contact radius, a, has acceptable literature values.[39] The proton dissociation rate constant, k_{PT}, is determined from the exponential decay at early times of the fluorescence decay. Over longer times, the fluorescence decay is nonexponential due to the reversible geminate recombination.

An important parameter in our model that strongly influences the nonexponential decay is the mutual diffusion coefficient, $D = D_{H^+} + D_{RO^-}$. The pressure dependence of the proton diffusion constant, D_{H^+}, for water as a function of pressure was measured by Nakahara and Osugi.[40] The proton conductivity slightly increases with pressure. The anion diffusion constant, D_{RO^-}, as a function of pressure, was estimated from the water viscosity dependence on pressure data.[41] At 20 °C, the viscosity slightly decreases at low pressures. At high pressure (>2 kbar), the viscosity slightly increases. At higher temperatures, the viscosity increases with pressure. Figure 1 shows the viscosity dependence on pressure of water at 303 K taken from ref 41. For comparison, we also display the viscosity dependence on pressure in ethanol and propanol.[41,42] Ethanol and propanol exhibit a much stronger pressure dependence of the viscosity. Another important parameter in the model is the Coulomb potential between the anion RO^-* and the geminate proton.

$$V(r) = -\frac{R_D}{r}; \quad R_D = \frac{|z_1 z_2| e^2}{\epsilon_0 k_B T} \tag{1}$$

where R_D is the Debye radius, z_1 and z_2 are the charges of the proton and anion, ϵ_0 is the static dielectric constant of the solvent, and T is the absolute temperature. e is the electronic charge, and k_B is Boltzmann's constant. We are not aware of published data of the change in the dielectric constant of water with pressure. In ethanol, it increases with pressure.[41] For calculation purposes of $V(r)$, we assume that the dielectric constant changes only slightly with an increase in pressure.

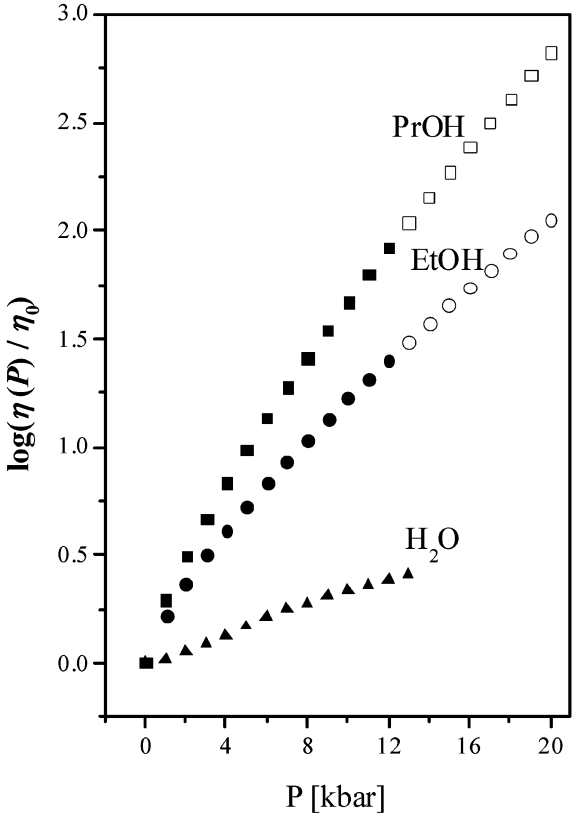

Figure 1. Viscosity dependence on the pressure of water, ethanol, and propanol at 303 K taken from refs 41 and 42. ■, propanol data; ●, ethanol data; ▲, water; open symbols are extrapolation to high pressure.

The asymptotic expression (the long time behavior) for the fluorescence of ROH*(t) is given by[38,43]

$$[ROH^*] \cong \frac{\pi}{2} a^2 \exp(R_D/a) \frac{k_r}{k_{PT}(\pi D)^{3/2}} t^{-3/2} \tag{2}$$

Equation 2 shows that uncertainty in the determination of $D(P)$ causes a larger uncertainty in k_r. Also, the fluorescence "background", due to a fluorescent impurity and the band overlap prevent us from accurately determining the recombination rate constant. We estimate that the error in the determination of k_{PT} is 10%. The error in the determination of k_{PT} is due to (1) the signal-to-noise ratio of the experimental signal, which affects the quality of the fluorescence signal over longer times and (2) the interplay between k_{PT} and k_r (see eq 2) over longer times. The uncertainty in the determination of k_r is estimated to be much larger, ~50%. The relatively large uncertainty in the values of k_r arises from the relation between k_r, $D(P)$, and ϵ(P). In this paper, we focus our attention on the pressure dependence of the proton dissociation rate constant, $k_{PT}(P)$, which is measured quite accurately.

2-Naphthol and 2-naphthol monosulfonate derivatives are relatively weak photoacids. The rate of proton transfer to water at atmospheric pressure at room temperature of these photoacids is relatively slow. For 2-naphthol in water, the excited lifetime is about 10 ns and the proton-transfer rate constant is of about the same order 10^8 s^{-1}. The most frequently cited values for the deprotonation rate constant k_d for 2-naphthol at room temperature are $7.0-7.5 \times 10^7$ s^{-1}, although 11×10^7 s^{-1} was used by Lee et al.,[44] and values between 30×10^7 s^{-1} and 5×10^7 s^{-1} have also been reported. Fox and co-workers results[31] at room temperature were consistent with the value of 7×10^7

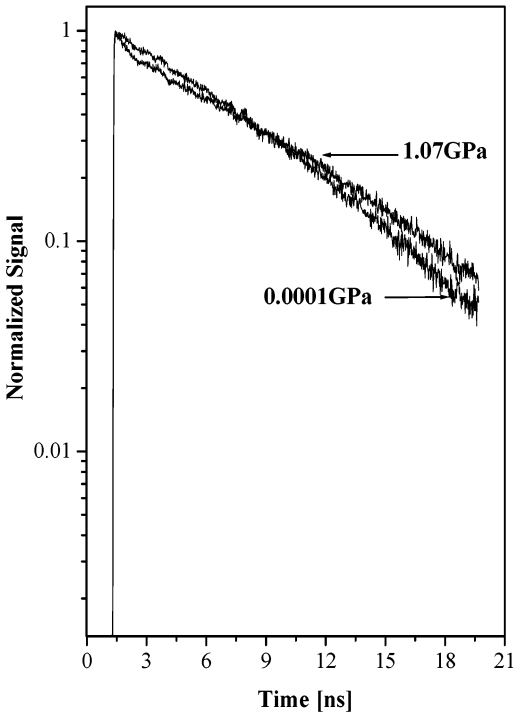

Figure 2. Semilog plot of the time-resolved emission intensity versus time of 2-naphthol in neat ethanol solution at several hydrostatic pressures.

TABLE 1: Excited State Lifetime of 2-Naphthol in Ethanol Solution

P^a [GPa]	τ_f [ns]^b	$a_f{}^c$	τ_S [ns]^d	$a_S{}^e$
0.0001	7.8410	0.989	0.4322	0.011
0.516	9.4671	0.986	0.2982	0.014
0.750	9.7350	0.983	0.6298	0.017
1.075	9.3846	0.981	0.4905	0.019
1.770	8.7260	0.966	0.8049	0.034

[a] 1 Gpa ~ 10 kbar. [b] τ_f is the fluorescence lifetime emission. [c] a_f is the amplitude of the long lifetime component. [d] τ_S is the short lifetime component of the emission. [e] a_S is the amplitude of the short lifetime component.

s^{-1}. We used the value of Lee et el.[44] for the proton-transfer rate at 1 atm.

2-Naphthol and its monosulfonate derivates are incapable of transferring protons to solvents that are weak bases, like alcohols (methanol and longer chain monols). To avoid ambiguity between the pressure effect on proton transfer and its effect on the excited state lifetime, we measured separately the excited-state lifetime, τ_f, of ROH* species as a function of pressure for 2-naphthol in ethanol solutions. Figure 2 shows the time-resolved emission measured at 360 nm of 2-naphthol in ethanol at atmospheric pressure and at 1.07 GPa. The measured lifetimes at various pressures, deduced from the fit of the emission curves, are given in Table 1. We used a multiexponential fit to the emission curves. The long lifetime component τ_f (see Table 1) has an amplitude of about 99% and is attributed to the excited state lifetime. At relatively low pressures, $P \leq 1$ GPa, the measured excited state lifetime increases slightly as a function of pressure. At high pressures, $P > 1.3$ GPa, the lifetime decreases slightly. The solution at atmospheric pressure contained oxygen and the lifetime increase at high pressure in ethanol solution can be attributed to a decrease in the oxygen concentration as a function of pressure.

In water solution, proton-transfer reaction occurs within the excited-state lifetime and the overall affect is a decrease in the observed emission lifetime of the ROH* band at 360 nm and the generation of a RO^-* band emitting at a maximum of 420 nm. The RO^-* time-resolved emission has a growth time which corresponds to the ROH* emission decay time.

Figure 3 shows, on a semilog scale, the experimental time-resolved emission intensity data of 2-naphthol, 2-naphthol-7-sulfonate, 2-naphthol-8-sulfonate, 2-naphthol, and 2-naphthol-6-sulfonate taken from ref 30, in water, measured at 350 nm at various pressures in the range of 0.001−11 kbar. The experimental data are shown by symbols and the computer fit by solid lines. We determined the proton-transfer rate constant, k_{PT}, from the fit to the initial decay of the ROH* fluorescence (~200 ps for 2-naphthol-8-sulfonate in water at 1 atm, at 298 K). The initial decay is mainly determined by the deprotonation process and is almost insensitive to the geminate recombination process. The long time behavior (the fluorescence tail) seen in the ROH* time-resolved emission is a consequence of the repopulation of the ROH* species by the reversible recombination of RO^-* with the geminate proton. The reprotonation of the excited ROH* can undergo a second cycle of deprotonation. The overall effect is a nonexponential fluorescence tail.[37] As seen in the figure, over the pressure range 0.001−10 kbar, the decay rate of the fluorescence increases as the pressure increases. The proton-transfer rate constant, k_{PT}, increases with pressure. Figure 4 shows, on a semilog scale, the experimental time-resolved emission measured at 435 nm, at about the ROH* band maximum (441 nm) of HPTS in water at various pressures, along with the computer fit (solid line).

Figure 5 shows the time-resolved emission of the 2-naphthol-8-sulfonate RO^-* species in water measured at 450 nm at atmospheric pressure and at 5.8 kbar, along with the computer fit (solid line) using the reversible proton-transfer model. The parameters used in the fit of RO^-* luminescence are extracted from the fit of the fluorescence decay curves of the ROH* species, measured at 350 nm. The emission intensity at 450 nm has a growth time, which corresponds to the proton transfer rate from the 2-naphthol ROH* species to water. Figure 5 clearly shows the growth time decrease as the pressure increases. The radiative decay times of the excited-state RO^-* are only slightly dependent on the pressure.

Our fit results for the proton-transfer rate to the solvent, $k_{PT}(P)$, as a function of pressure for 2-naphthol, 2-naphthol-7-sulfonate, 2-naphthol-8-sulfonate, and HPTS are summarized in Tables 2−5, respectively.

Discussion

In the following section, we first present the basic theoretical concepts related to nonadiabatic and adiabatic proton transfers. This is followed by a description of our stepwise two coordinate proton-transfer model accounting for both the temperature and pressure dependence of the proton-transfer rate. Finally, we fit the experimental results to our model for proton transfer.

The theory for nonadiabatic proton transfer is very similar to the theory for nonadiabatic electron transfer in its treatment of the involvement of the solvent. In the model,[18] when the polar solvent is equilibrated to the reactant, the proton will not be transferred due to an energy mismatch in the reactant and product states. Upon solvent fluctuation, the energy of the reactant and product states becomes equal and it is in this solvent configuration that the proton tunnels from one side of the well to the other. Finally, upon solvent relaxation, the product state is formed.

If the pretunneling and posttunneling configurations are regarded as real, transient intermediates, the process can be

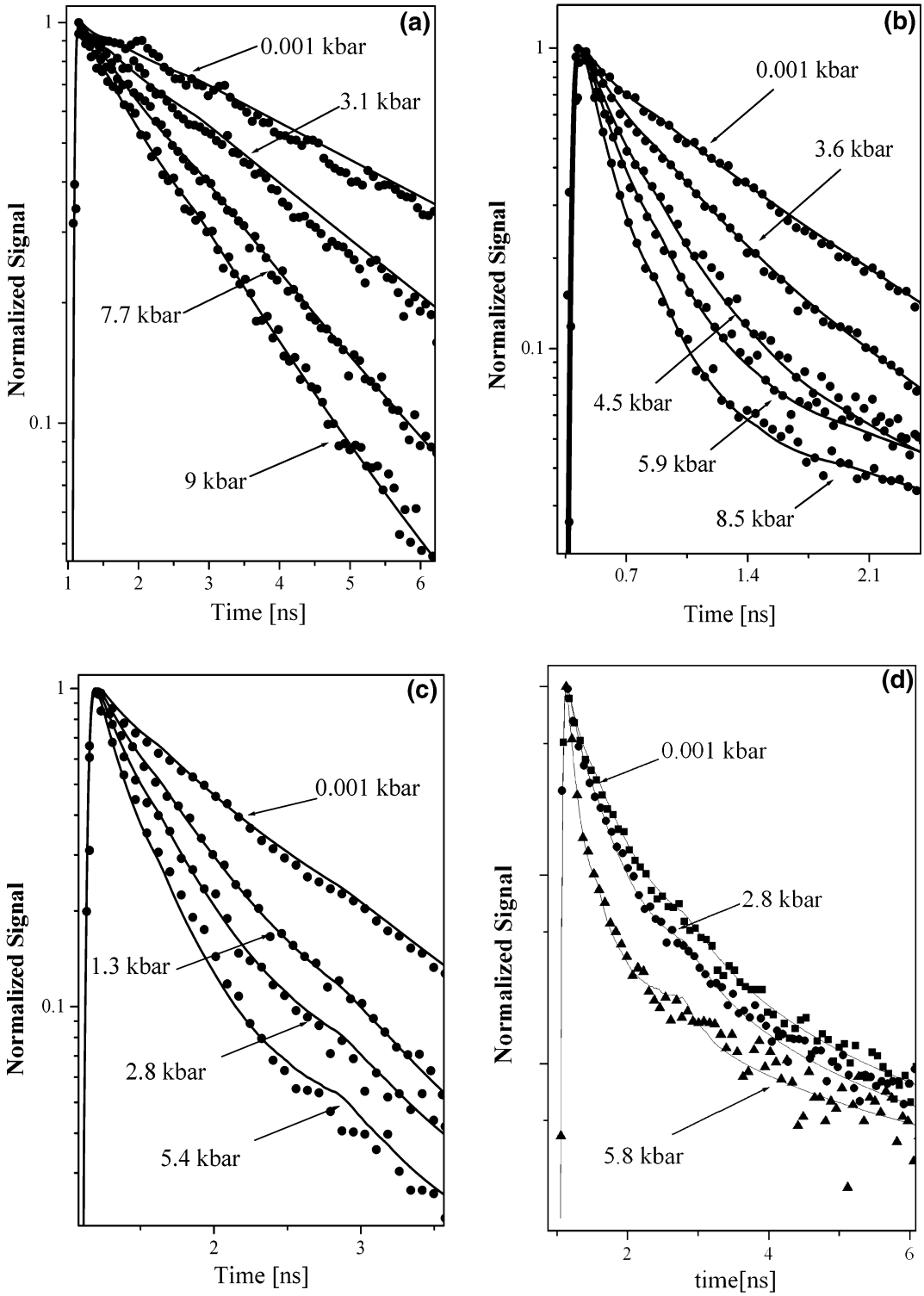

Figure 3. Experimental time-resolved emission intensity data (symbol) in water solution measured at 350 nm at various pressures in the range of 0.001−11.6 kbar along with the computer fit (solid lines), semilog scale of a. 2-naphthol, b. 2-naphthol-6-sulfonate, c. 2-naphthol-7-sulfonate, and d. 2-naphthol-8-sulfonate.

described by a set of three consecutive chemical equations[45] given in Scheme 2, along with a qualitative description of the potential surfaces along the solvent coordinate, *S*, and the proton coordinate q_H, where AH is the protonated photoacid, S_B is a single solvent molecule to which the proton is transferred, S_R is the solvent configuration to stabilize the reactants, and S_p is the solvent configuration of the products. $S^{\ddagger}$ is the solvent configuration to equally stabilize $AH\cdots S_B$ and $A^-\cdots HS_B^+$. The first equation describes the motion along the solvent configuration coordinate in the reactant potential surface, denoted as *R*, to reach the activated solvent configuration. The second equation describes the tunneling process in the proton coordinate, q_H. This process occurs only when the energy of the reactant and product states becomes equal, at $S^{\ddagger}$. The third equation describes the solvent configuration relaxation toward the bottom of the product well, denoted as *P*.

One important difference between electron transfer and proton transfer is the extreme sensitivity of the proton tunneling matrix element to distance. The functional form of the tunneling coupling matrix element between the reactant and

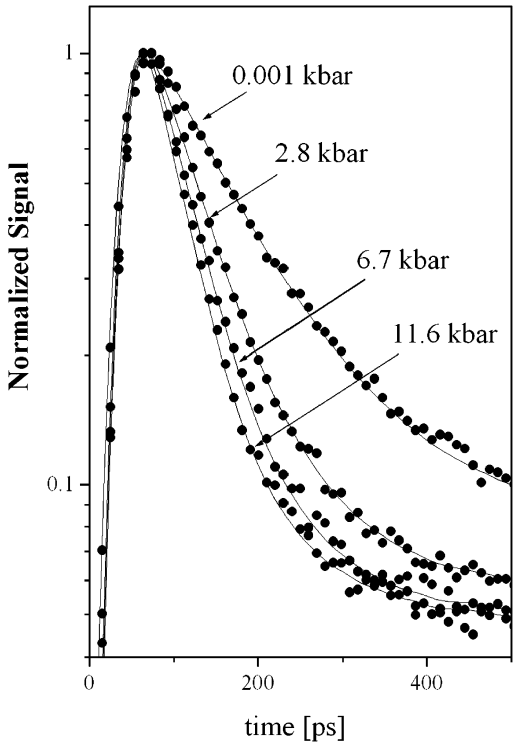

Figure 4. Experimental time-resolved emission measured at 435 nm (symbol) of HPTS in water at various pressures in the range of 0.001−11.6 kbar along with the computer fit (solid lines), semilog scale.

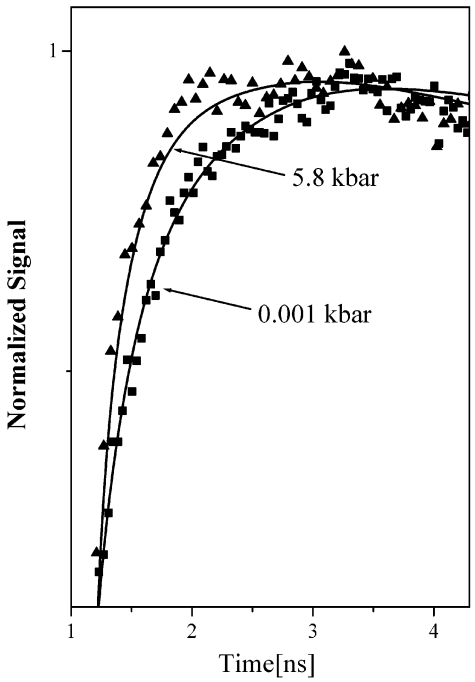

Figure 5. Time-resolved emission of 2-naphthol-8-sulfonate RO^{-}* species in a water solution measured at 450 nm (symbol) at atmospheric pressure and 5.8 kbar along with the computer fit (solid lines), semilog scale.

product state, for moderate to weak coupling, is

$$C(q_H) = C_0 \exp(-\alpha_P \delta q_H) \qquad (3)$$

The decay parameter, α, is very large, 25−35 $Å^{-1}$, in comparison with the corresponding decay parameter for the electronic coupling in electron transfer, 1 $Å^{-1}$. It is this feature that makes the dynamics of proton transfer so sensitive to the internuclear separation of the two heavy atoms, and hence, pressure can be used to gradually change the intermolecular distance. For many liquids, the pressure is known to change the liquid and solid density. For ethanol, the volume decreases by about 25% at about 10 kbar. As the volume decreases with pressure, so does the intermolecular distance. Water compressibility is relatively low, at 10 kbar it changes by only 15%. Figure 6 shows the dependence of $1/\alpha_P = V_P/V_0$ on pressure, for water. For comparison, we also added the pressure dependence of $1/\alpha_P$ for ethanol and propanol, where V_P values for

TABLE 2: Pressure Dependence of the Kinetic Parameters for the Proton Transfer Reaction of 2-Naphthol in H_2O

$P^{a,b}$ [GPa]	$k_{PT}{}^{c}$ [10^9 s^{-1}]	$k_{PT}(P)/k_{PT}(1\ atm)^{c}$	$k_r{}^{c,d}$ [10^9 Å s^{-1}]
0.0001	0.125	1.00	10.0
0.31	0.26	2.08	10.0
0.77	0.64	0.64	20.0
0.90	0.85	5.12	20.0
1.16	1.00	6.8	10.0

[a] 1 Gpa ∼ 10 kbar. [b] The error in determination of the pressure is ±0.075 Gpa. [c] k_{PT} and k_r are obtained from the fit of the experimental data by the reversible proton-transfer model (see text). [d] The error in the determination of k_r is 50%, see text.

TABLE 3: Pressure Dependence of the Kinetic Parameters for the Proton Transfer Reaction of 2N7S in H_2O

$P^{a,b}$ [GPa]	$k_{PT}{}^{c}$ [10^9 s^{-1}]	$k_{PT}(P)/k_{PT}(1\ atm)^{c}$	$k_r{}^{c,d}$ [10^9 Å s^{-1}]
0.0001	1.15	1.00	13.0
0.13	2.10	1.83	15.0
0.28	3.70	3.22	16.5
0.54	5.60	4.87	22.0
0.75	6.60	5.74	23.0
0.80	8.45	7.34	23.0
0.88	9.20	8.00	23.0
1.02	9.8	8.52	23.0
1.12	10.3	8.97	25.0

[a] 1 Gpa ∼ 10 kbar. [b] The error in determination of the pressure is ±0.075 Gpa. [c] k_{PT} and k_r are obtained from the fit of the experimental data by the reversible proton-transfer model (see text). [d] The error in the determination of k_r is 50%, see text.

TABLE 4: Pressure Dependence of the Kinetic Parameters for the Proton Transfer Reaction of 2N8S in H_2O

$P^{a,b}$ [GPa]	$k_{PT}{}^{c}$ [10^9 s^{-1}]	$k_{PT}(P)/k_{PT}(1\ atm)^{c}$	$k_r{}^{c,d}$ [10^9 Å s^{-1}]
0.0001	4.0	1.00	30.0
0.20	6.0	1.33	30.0
0.58	18.0	4.00	30.0
0.67	20.0	4.44	30.0
0.80	24.0	5.33	34.0
1.2	30.0	6.67	42.0

[a] 1 Gpa ∼ 10 kbar. [b] The error in determination of the pressure is ±0.075 Gpa. [c] k_{PT} and k_r are obtained from the fit of the experimental data by the reversible proton-transfer model (see text). [d] The error in the determination of k_r is 50%, see text.

TABLE 5: Pressure Dependence of the Kinetic Parameters for the Proton Transfer Reaction of HPTS in H_2O

$P^{a,b}$ [GPa]	$k_{PT}{}^{c}$ [10^9 s^{-1}]	$k_{PT}(P)/k_{PT}(1\ atm)^{c}$	$k_r{}^{c,d}$ [10^9 Å s^{-1}]
0.0001	9.3	1.00	7.75
0.28	19.2	2.06	8.40
0.54	22.0	2.37	9.00
0.67	26.0	2.80	10.00
0.96	28.7	3.09	11.00
1.16	32.0	3.44	11.50

[a] 1 Gpa ∼ 10 kbar. [b] The error in determination of the pressure is ±0.075 Gpa. [c] k_{PT} and k_r are obtained from the fit of the experimental data by the reversible proton-transfer model (see text). [d] The error in the determination of k_r is 50%, see text.

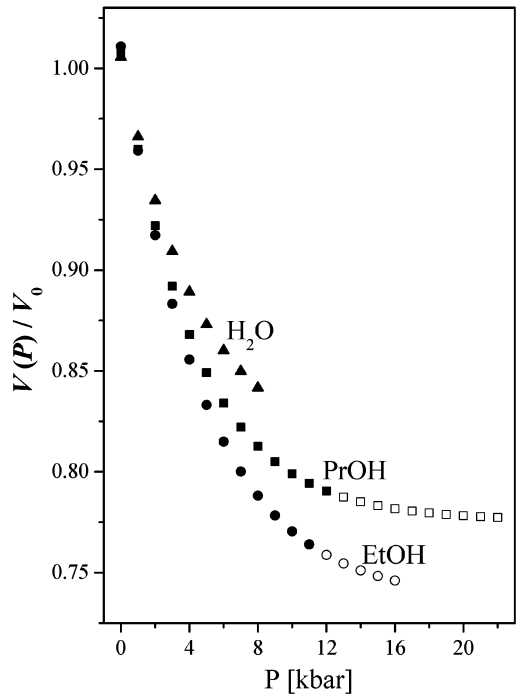

Figure 6. Pressure dependence of $1/\alpha_P = V_P/V_0$ of water, ethanol, and propanol.

SCHEME 2

(a) $AH+S_B+S_R \underset{k_{-1}}{\overset{k_1}{\rightleftharpoons}} AH\cdot S_B+S^{\neq}$

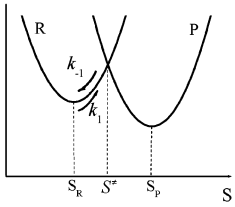

(b) $AH\cdot S_B+S^{\neq} \underset{k_{-2}}{\overset{k_2}{\rightleftharpoons}} A^-\cdot HS_B^+ + S^{\neq}$

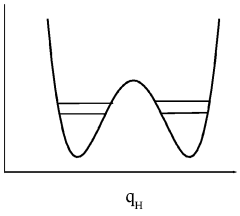

(c) $A^-\cdot HS_B^+ + S^{\neq} \xrightarrow{k_3} A^- + HS_B^+ + S_p$

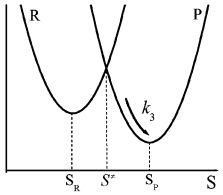

both liquids are taken from ref 41. The compressibility, $1/V(\partial V/\partial P)_T$, is a function of P. As seen in Figure 5, the compressibility decreases with pressure. In general, it is smaller for water than methanol and ethanol. For water and ethanol, it changes by a factor of about 3 and 5 between atmospheric pressure and 10 kbar, respectively. As a first-order approximation, the change in intermolecular distance, δq_H, is related to the change in volume ΔV as $(\Delta V)^{1/3}$. In the strong coupling limit, the tunneling matrix element, C, varies much less rapidly with changing q_H and is approximately linear.

Qualitative Model for the Temperature and Pressure Dependencies of Excited-State Proton-Transfer Reactions. Previously, we used a qualitative model that accounts for both the temperature[9−12] and, recently,[28−30] pressure dependences of the excited-state intermolecular proton transfer to the solvents water, ethanol, and propanol. We shall use the same model to explain the large pressure dependence of the proton-transfer rate from 2-naphthol, 2-naphthol-7-sulfonate, and 2-naphthol-8-sulfonate to water. As described in the Introduction, the proton-transfer reaction depends on two coordinates, the first of which depends on the generalized solvent configuration. The solvent coordinate characteristic time, τ_S, is within the range of the dielectric relaxation time, τ_D, and τ_L, the longitudinal relaxation time. The second coordinate is the actual proton translational motion (tunneling) along the reaction path, q_H.

In the stepwise model, the overall proton-transfer time is the sum of two times, $\tau = \tau_S + \tau_H$, where τ_S is the characteristic time for the solvent reorganization and τ_H the time for the proton to pass to the acceptor. The overall rate constant, k_{PT}, at a given temperature, T, and pressure, P, is given by

$$k_{PT}(T,P) = \frac{k_H(T,P)k_S(T,P)}{k_H(T,P) + k_S(T,P)} \tag{4}$$

where $k_S(T,P)$ is the solvent coordinate rate constant and $k_H(T,P)$ the proton coordinate rate constant. Equation 4 provides the overall excited-state proton-transfer rate constant along the lines of a stepwise process. Our stepwise model[10−14] for the overall proton-transfer rate constant expression (eq 4) is similar to the expression of Rips and Jortner[46] for the overall ET rate constant that bridges between the two extreme cases: the nonadiabatic and adiabatic ET. The model restricts the proton transfer process to a stepwise one. The proton moves to the adjacent hydrogen bonded solvent molecule only when the solvent configuration brings the system to the crossing point. As a solvent coordinate rate constant, we use

$$k_S(T,P) = b\frac{1}{\tau_D(T,P)}\exp\left(-\frac{\Delta G^{\ddagger}}{RT}\right) \tag{5}$$

where b is an adjustable empirical factor determined from the computer fit of the experimental data. We find that the empirical factor for monols lies between 2 and 4, whereas for water, it is larger and lies in the range 4−8. For the monols, τ_L is usually smaller than τ_D by a factor of 2−6 and, for water, by about a factor of 10. Thus, the solvent characteristic time, $\tau_S = 1/k_S(T,P)$, for water and monols lies between the dielectric relaxation and longitudinal times, $\tau_L < \tau_S < \tau_D$. The activation energy, $\Delta G^{\ddagger}$, is determined by the Marcus relation

$$\Delta G^{\ddagger} = \frac{1}{4E_S}(E_S + \Delta G)^2 \tag{6}$$

where E_S is the solvent reorganization energy and ΔG is the free energy of the reaction. Thus, one needs to know the excited-state acid equilibrium constant, K_a^*, and the solvent reorganization energy. An alternative expression for $\Delta G^{\ddagger}$ can be evaluated from the structure reactivity relation of Agmon and Levine.[47] In our treatment, we assume that $\Delta G^{\ddagger}$ is independent of the hydrostatic pressure and hence the pressure solely affects the preexponential factor. In a previous study on the temperature dependence of the proton-transfer rate from photoacids to water,[14] we found the activation energies for 2-naphthol ($pK^* = 2.7$) and 2-naphthol-6,8-disulfonate ($pK^* = 0.4$) to be $\Delta G^{\ddagger} = 10$ and 2.5 kJ/mol, respectively. These values agree qualitatively with the Marcus expression for the activation energy (see eq 6) assuming reorganization energies in the range of 0.1−

0.3 eV. The pK_a^* value of 2-naphthol-7-sulfonate and 2-naphthol-8-sulfonate is between that of the two compounds mentioned above, $pK_a^* \approx 1.7$ and ~ 1, respectively. We therefore estimate the activation energy value for those two compounds to be $\Delta G^{\ddagger} \approx 6$ and 3.5 kJ/mol, respectively. The reaction rate constant, k_H, along the proton coordinate, q_H, is expressed by the usual activated chemical reaction description given by

$$k_H(P) = k_H^0(P) \exp\left(-\frac{\Delta G^{\ddagger}}{RT}\right) \quad (7)$$

where $k_H^0(P)$ is a pressure-dependent preexponential factor. For monols, at high enough temperature or in the case of solvents with a large relaxation rate (which is the case of water, $\tau_D = 8$ ps), the actual proton transfer along the proton tunneling coordinate, q_H, is the slower process and, hence, the rate determining step. This rate strongly depends on pressure since tunneling in the intermediate coupling case depends exponentially on the intermolecular distance between the two heavy atoms. In this comparative study of naphthol, naphthol monosulfonate derivatives, and HPTS, the proton transfer occurs between the hydroxyl group of the photoacid and the adjacent oxygen of a hydrogen bonded water molecule.

As we shall show in the next section, $k_H(P)$ is related to the nonadiabatic limit rate expression. In the nonadiabatic limit, the preexponential factor, is related to the tunneling coupling matrix element (see eq 6). The coupling matrix element depends strongly on the pressure and increases as the pressure increases.

Bromberg et al.[48] studied the effect of pressure and temperature on the photoinduced hydrogen transfer reaction in a mixed crystal of acridine in fluorene. The room temperature hydrogen transfer rate increases exponentially when pressure increases. Based on proton tunneling concepts, Trakhtenberg and Klochikhin[26] derived an expression for the pressure and temperature dependence of the tunneling rate of proton transfer in the solid state

$$k(P,T) = \nu \exp[-J(R_0) + J'R_0(1 - \alpha_P^{-1/3}) + J'^2\delta_{CN}^2/8\alpha_P^{\gamma} \coth(\hbar\Omega_0\alpha_P^{\gamma}/4k_BT)] \quad (8)$$

where $\alpha_P(P) = V_0/V(P)$, Ω_0 is the effective frequency of the intermolecular vibration, δ_{CN}^2 is the square of the amplitude of the intercenter C···N distance, and $\gamma = -\partial \ln \Omega_0/\partial \ln V$

$$J(R) = (2/\hbar) \int \{2m[U(x,R) - E_H(R)]\}^{1/2} \, dx \quad (9)$$

$E_H(R)$ and $U(x,R)$ are the total and potential energies of the tunneling atom respectively, depending on the distance, R, between the two heavy atoms (in our case two oxygen atoms). R_0 is the equilibrium distance between the heavy atoms and J' the derivative, $\partial J/\partial R$. The first term on the right-hand side of eq 8 is the tunneling expression at atmospheric pressure and does not account for the pressure effect. The second term accounts for the change in the tunneling rate with pressure due to the change in the distance between the two heavy atoms. The third term takes into account the pressure effect on the intermolecular low-frequency modulation Ω_0. Trakhtenberg et al.[26] found good correspondence with the experimental results of Bromberg et al.[48] when they used a smaller power dependence of the compressibility, α_P (0.22 instead of 1/3 as expected from the relation of distance and volume).

In our previous pressure studies of DCN2 in ethanol and propanol, we estimated the pressure dependence of the proton coordinate rate constant, $k_H(P)$, from the second term of eq 8 with a compressibility dependence on power of 0.22 for ethanol and 0.27 for propanol.[28,29] For all of the photoacid−water systems discussed here, we used the value of 0.33[30] since, for the first approximation, $\delta q_H = (\Delta V)^{1/3}$. The contribution of the third term in eq 8 is rather small. For $\Omega_0 = 5.0 \times 10^{13}$ s^{-1}, $\delta_{O-O}^2 = 0.005$ Å^2, $\alpha_P = 1/3$, and $\gamma = 0.22$ (see ref 25), we find that the third term in eq 8 decreases the tunneling rate as the pressure increase. The rate decreases by about 30% at about 10 kbar. At higher pressures, the value of the third term is about the same as at 10 kbar since the volume compressibility is very small at high pressures. In our treatment, we neglected the contribution to the pressure dependence of the third term in eq 8. Thus, the change in the proton tunneling rate constant as a function of pressure is given by

$$\frac{k_H(P)}{k_H(1 \text{ atm})} \cong \exp[J'R_0(1 - \alpha_P^{-0.33})] \quad (10)$$

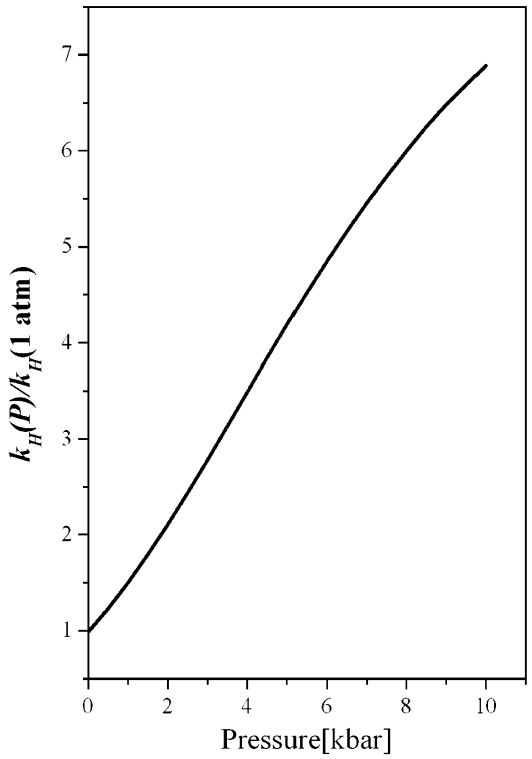

Figure 7. Pressure dependence of the proton tunneling rate constant, using eq 8. parameters $J' = 14.2$ Å^{-1}, $R_0 = 2.4$ Å, and α_P, was taken from refs 41 and 55.

Figure 7 shows the pressure dependence of the proton tunneling rate constant, using eq 10, and the following parameters, $J' = 14.2$ Å^{-1}, $R_0 = 2.4$ Å, and $J'R_0 = 34$. α_P was taken from ref 41. As seen, the rate increases as a function of pressure. Since $1/\alpha_P$ is not constant with pressure, but rather decreases as the pressure increases, $k_H(P)/k_H(1 \text{ atm})$ does not increase with the same initial slope.

In previous studies[9−14] we used the longest component of the dielectric relaxation time, τ_D, for the solvent coordinate preexponential factor of the rate constant, $k_S = b/\tau_D \exp(-\Delta G^{\ddagger}/RT)$, where b is an empirical factor. For water, we found $b \approx 6$ and for all monols studied the value is less, $2 < b < 4$. The pressure dependence of the dielectric relaxation time up to about $\sim$1 kbar was measured by Pottel and Asselborn.[49]

Free energy relation[50−52] and temperature dependence experiments[11] indicate that the solvent fluctuation rate to equalize the energies is not in the high-frequency range of the order of 10^{13}

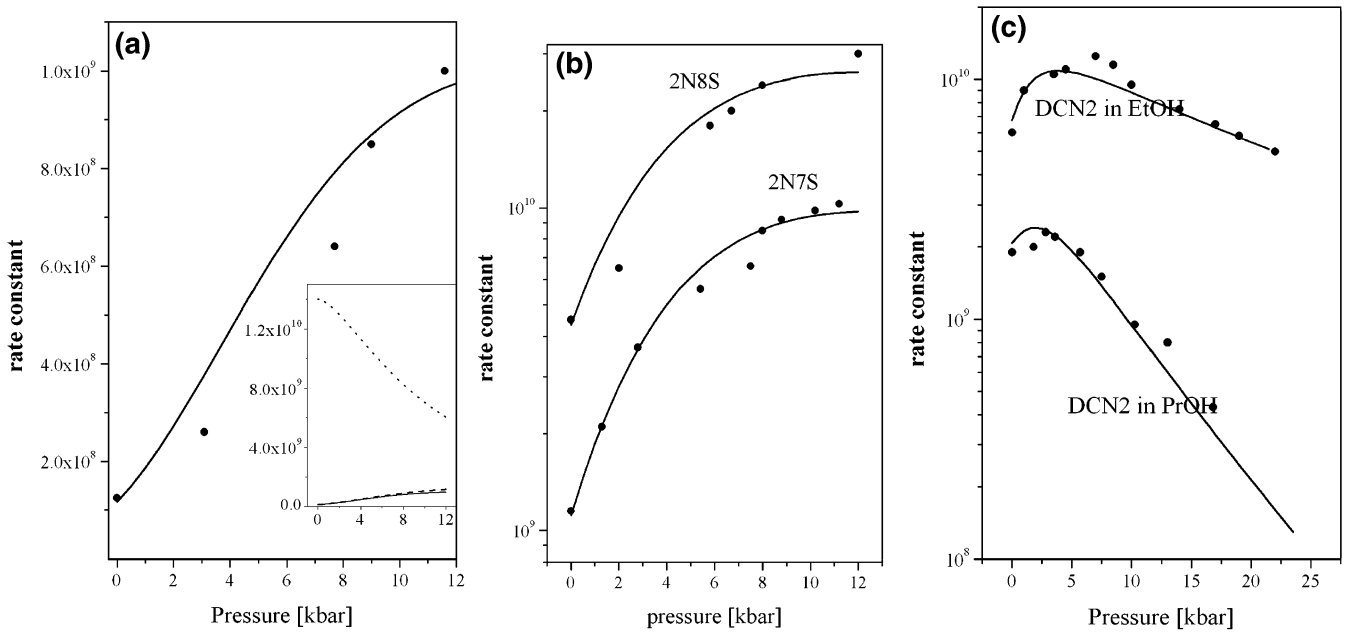

Figure 8. Fit to the stepwise two coordinate model of $k_{PT}(P) = [k_H(P)k_S(P)]/[k_H(P) + k_S(P)]$ as a function of pressure (solid line) along with the experimental data (dots). a. 2-Naphthol in water. $k_H(P)$ and $k_S(P)$ are shown as dashed and dotted lines, respectively. Inset: calculated rate constants. b. 2N7S and 2N8S in water, semilog scale. c. DCN2 in ethanol[28] and propanol,[30] semilog scale.

s^{-1} (~100−200 cm^{-1}) but rather slower than 10^{12} s^{-1}, (<10 cm^{-1}). For monols, diols and glycerol, it is very close to $1/\tau_D$, where τ_D is the slow component of the dielectric relaxation time. For water, the solvent fluctuation rate is higher, about 6 times larger than $1/\tau_D$ (water). The dielectric relaxation only slightly increases with pressure over this limited range. It is about 15% slower at 1 kbar than at atmospheric pressure. We are not aware of literature-published values for the dielectric relaxation times as a function of pressure for water at higher pressures up to the freezing pressure of ~11 kbar. In many cases, the viscosity and τ_D have similar dependencies on both pressure and temperature. As seen in Figure 1, the viscosity dependence on the pressure of water at 30 °C is very mild, whereas in ethanol and propanol, the dependence is much larger.

The dielectric relaxation time is often directly proportional to the shear viscosity. This is a direct consequence of the assumed viscous-damped rotating sphere model of dielectric relaxation originally introduced by Debye.[39] In general, the viscosity dependence on pressure is larger than that of the dielectric relaxation. Johari and Danhauser studied the pressure dependence of the viscosity and the dielectric relaxation of isomeric octanols.[53,54] They found good correspondence between the pressure dependence of the viscosity and dielectric relaxation times.

We used an approximate relation between $\tau_D(P)$ and $\eta(P)$ based on the correspondence between dielectric relaxation and $\eta(P)$ to estimate the pressure dependence of the $\tau_D(P)$ of water

$$\tau_D(P) \sim \tau_D^{1atm}\left(\frac{\eta(P)}{\eta^{1atm}}\right)\exp(-P/P^*) \qquad (11)$$

For the best fit to the pressure dependence of k_{PT} using our stepwise model, we used $P^* = 4500$ bar.

Figure 8a shows a fit to the stepwise two coordinate model of $k_{PT}(P) = [k_H(P)k_S(P)]/[k_H(P) + k_S(P)]$ as a function of pressure (solid line) along with the experimental data (dots) of 2-naphthol in water. Figure 8b shows the fit and experimental results of the proton-transfer rate for both 2N7S and 2N8S. The results of 2-naphthol and 2-naphthol monosulfonate derivatives in water show a large increase of the proton-transfer rate with pressure changes. At about 11 kbar, the rate is 10-fold larger than the rate at atmospheric pressure. Table 6 gives the fitting parameters of the model for the proton-transfer rate of these compounds in water. The values of the parameters $J'R_0$ (see eq 10) range from 35 to 40. The value of the solvent relaxation parameter $b = 5$ for all calculations. In Figure 8c, we also show, for comparison, the pressure dependence of DCN2 in ethanol and propanol taken from our previous studies.[28,29] The results of DCN2 in ethanol show an initial increase of the rate with the pressure. At about 8 kbar, the rate reaches a maximum value, $k_{PT}(8\text{ kbar}) = 2k_{PT}(1\text{ atm})$. Further pressure increase, decreases the proton-transfer rate constant to the solvent. This interesting pressure dependence observation of the proton-transfer rate from DCN2 to ethanol is explained by the opposite pressure dependencies of k_H and k_S and the saturation of k_H at medium-pressure values. The results of DCN2 in propanol show a slight increase of the proton-transfer rate with pressure changes up to about 5 kbar. At pressures above 5 kbar (0.5 GPa), the rate decreases as a function of pressure. At 5 kbar, the rate is 20% larger than the value at atmospheric pressure, whereas at higher pressures, up to ~2.5 GPa (25 kbar), the proton-transfer rate decreases with pressure and its value is related to the inverse of the dielectric relaxation time. At about 2.2 GPa, the rate is smaller, by a factor of about 20, than that at atmospheric pressure. The pressure dependence of k_H and k_S for 2-naphthol in water are also plotted (dotted lines) in Figure 8a. The explanation for the large difference in the pressure dependence of the proton-transfer rate from 2-naphthol and the derivatives to water and that from DCN2 to ethanol and propanol is given along the lines of the stepwise, two coordinates proton-transfer model.

TABLE 6: Parameters for the Proton Transfer Rate Fittings

photoacid	$J'R_0$	$\Delta G^{\ddagger}$ [kJ/mol]	k_H(1atm) [ns^{-1}]
2-naphthol	36	10	0.012
2N6S	35	6.0	0.9
2N7S	40	6.0	1.15
2N8S	35	3.5	4.5
HPTS	29	3.5	10.5

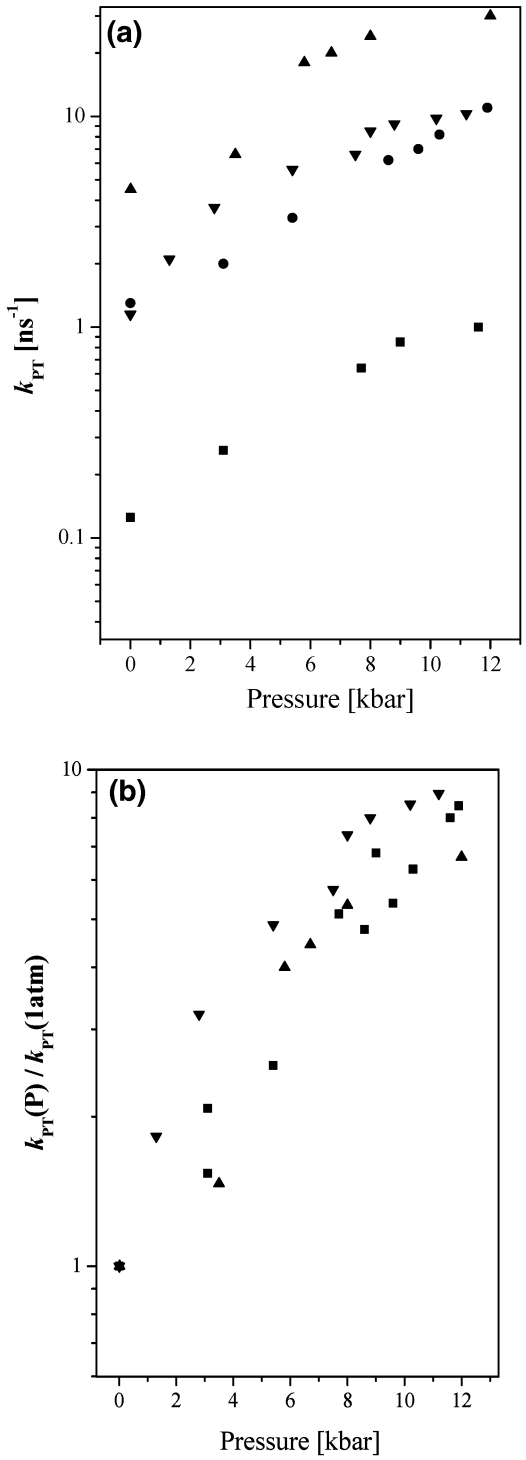

Figure 9. k_{PT}, as a function of pressure, for 4 different photoacids in water, semilog scale: 2-naphthol, ■; 2N6S, ●; 2N7S, ▼; 2N8S, ▲; a. k_{PT}(P) [ns^{-1}], b. k_{PT}(P)/k_{PT}(1atm).

Figure 9a shows, on a semilog plot, the proton-transfer rate constant, k_{PT}, and Figure 9b shows these rates, normalized by the rate at 1 atm [$k_{PT}(P)/k_{PT}$(1atm)], as a function of pressure for 2N, 2N6S (taken from ref 30), 2N7S, and 2N8S. The relative change in the proton-transfer rate from the four photoacids, 2N, 2N6S, 2N7S, and 2N8S to water as a function of pressure is about the same within the errors involved in the determination of the pressure and the proton-transfer rate. The error in the determination of the pressure is ±0.075% GPa and the proton-transfer rate constant, k_{PT}, ±5%. The rate increases with pressure up to about the freezing point. For all proton emitters at about 10 kbar, the freezing point, it is larger by about a factor of 8 ±1 than that at atmospheric pressure. The small differences shown between the slopes of the various plots in Figure 9, probably arise from the errors in the experiment.

Unlike the pressure effect on proton transfer from these compounds to water, HPTS exhibits a much milder pressure effect. At about the freezing point, the rate is about 3 times larger than at atmospheric pressure. A plausible explanation for the milder pressure effect may arise from the large difference between the ring skeleton structure of the pyrene (compared with naphthol). Another possible explanation is the large negative electric charge of the three sulfonate groups of HPTS. The much larger charge of HPTS may influence the local water structure around the molecule. A fixation of a local water network around HPTS, due to electrostatic forces as well as hydrogen bonding, may decrease the pressure effect on proton transfer.

Summary

We studied, using time-resolved emission techniques, the proton dissociation and reversible geminate recombination from the photoacids 2-naphthol, 2-naphthol monosulfonate derivatives, and HPTS to water as a function of pressure. The experimental time-resolved fluorescence data are analyzed by the exact numerical solution of the transient Debye−Smoluchowski equation (DSE).

We found that the proton dissociation rate constant, k_{PT}, of those excited photoacids in water up to the pressure of the freezing point (∼ 11 kbar), increases by a factor of between 3 and 8 with pressure. We compared these results with our previous pressure work on DCN2 in ethanol and propanol.

We used a stepwise two coordinates model to qualitatively fit the pressure dependence of the proton transfer rate. We previously used this model to successfully explain the temperature and pressure dependences of the proton-transfer rate from various photoacids to solvents.[9−13,28] The analysis of the experimental data by the model shows that the pressure affects both steps but in opposite directions. In the case of proton transfer from 2-naphthol and naphthol monosulfonate derivatives to water, pressure only mildly affects the solvent coordinate rate, k_S. In contrast to k_S, the tunneling rate, k_H, increases almost 10-fold with pressure. The overall effect is a strong increase of the rate with pressure.

Acknowledgment. We thank Prof. M. Pasternak and Dr. G. Rozenberg for providing the diamond anvil cell high-pressure technology. This work was supported by grants from the U.S.−Israel Binational Science Foundation and the James-Franck German-Israel Program in Laser-Matter Interaction.

References and Notes

(1) Weller, A. *Prog. React. Kinet.* **1961**, *1*, 189.
(2) Förster, Th.; Volker, S. *Chem. Phys. Lett.* **1975**, *34*, 1.
(3) Ireland, J. F.; Wyatt, P. A. H. *Adv. Phys. Org. Chem.* **1976**, *12*, 131.
(4) Huppert, D.; Gutman, M.; Kaufmann, K. J. In *Advances in Chemical Physics*; Jortner, J., Levine, R. D., Rice, S. A., Eds.; Wiley: New York, 1981; Vol. 47, p 681. Kosower, E. M.; Huppert, D. In *Annual Reviews of Physical Chemistry*; Strauss, H. L., Babcok, G. T., Moore, C. B., Eds.; Annual Reviews Inc.: Palo Alto, CA, 1986; Vol. 37, p 122.
(5) Lee, J.; Robinson, G. W.; Webb, S. P.; Philips, L. A.; Clark, J. H. *J. Am. Chem. Soc.* **1986**, *108*, 6538.
(6) Gutman, M.; Nachliel, E. *Biochim. Biophys. Acta* **1990**, *391*, 1015.
(7) Knochenmuss, R. *Chem. Phys. Lett.* **1998**, *293*, 191.
(8) Peters, S.; Cashin, A.; Timbers, P. *J. Am. Chem. Soc.* **2000**, *122*, 107.
(9) Poles, E.; Cohen, B.; Huppert, D. *Israel J. Chem.* **1999**, *39*, 347.

(10) Cohen, B.; Huppert, D. *J. Phys. Chem. A* **2000**, *104*, 2663.
(11) Cohen, B.; Huppert, D. *J. Phys. Chem. A* **2001**, *105*, 2980.
(12) Cohen, B.; Huppert, D. *J. Phys. Chem.* **2002**, *106*, 1946−1955.
(13) Cohen, B.; Segal, J.; Huppert, D. J. *Phys. Chem. A* **2002**, *106*, 7462−7467.
(14) Cohen, B.; Leiderman, P.; Huppert, D. *Phys. Chem. A* **2002**, *106*, 11115−11122.
(15) Kolodney, E.; Huppert, D. *J. Chem. Phys.* **1981**, *63*, 401.
(16) Ando, K.; Hynes, J. T. In *Structure, energetics and reactivity in aqueous solution*; Cramer, C. J., Truhlar, D. G., Eds.; ACS Books: Washington, DC, 1994.
(17) Agmon, N.; Huppert, D.; Masad, A.; Pines, E. *J. Phys. Chem.* **1991**, *96*, 952.
(18) German, E. D.; Kuznetsov, A. M.; Dogonadze, R. R. *J. Chem. Soc., Faraday Trans. 2* **1980**, *76*, 1128.
(19) Kuznetsov, A. M. *Charge Transfer in Physics, Chemistry and Biology*; Gordon and Breach: New York, 1995.
(20) Borgis, D.; Hynes, J. T. *J. Phys. Chem.* **1996**, *100*, 1118. Borgis, D. C.; Lee, S.; Hynes, J. T. *Chem. Phys. Lett.* **1989**, *162*, 19. Borgis, D.; Hynes, J. T. *J. Chem. Phys.* **1991**, *94*, 3619.
(21) Kiefer, P. M.; Hynes, J. T. *Solid State Ionics* in press.
(22) Cukier, R. I.; Morillo, M. *J. Chem. Phys.* **1989**, *91*, 857. Morillo, M.; Cukier, R. I. *J. Chem. Phys.* **1990**, *92*, 4833.
(23) Li, D.; Voth, G. A. *J. Phys. Chem.* **1991**, *95*, 10425. Lobaugh, J.; Voth, G. A. *J. Chem. Phys.* **1994**, *100*, 3039.
(24) Hammes-Schiffer, S. *Acc. Chem. Res.* **2001**, *34*, 273.
(25) Ando, K.; Hynes, J. T. *J. Phys. Chem. B* **1997**, *101*, 10464.
(26) Trakhtenberg, L. I.; Klochikhin, V. L. *Chem. Phys.* **1998**, *232*, 175.
(27) Goldanskii, V. I.; Trakhtenberg, L. I.; Fleuorov, V. N. *Tunneling Phenomena in Chemical Physics*; Gordon and Breach: New York, 1989; Chapter IV.
(28) Koifman, N.; Cohen, B.; Huppert, D. *J. Phys. Chem. A* **2002**, *106*, 4336.
(29) Genosar, L.; Leiderman, P.; Koifman, N.; Huppert, D. *J. Phys. Chem. A* **2004**, *108*, 309.
(30) Leiderman, P.; Genosar, L.; Koifman, N.; Huppert, D. *J. Phys. Chem. A* **2004**, accepted.
(31) Green, S.; Xiang, T.; Johnston, K. P.; Fox, M. A. *J. Phys. Chem.* **1995**, *99*, 13787.
(32) Huppert, D.; Jayaraman, A.; Maines, R. G., Sr.; Steyert, D. W.; Rentzepis, P. M. *J. Chem. Phys.* **1984**, *81*, 5596.
(33) Jayaraman, A. *Rev. Mod. Phys.* **1983**, *55*, 65.
(34) Machavariani, G. Yu.; Pasternak, M. P.; Hearne, G. R.; Rozenberg, G. Kh. *Rev. Sci. Instrum.* **1998**, *69*, 1423.
(35) D'ANVILS is administered by Ramot Ltd., 32 H. Levanon Str., Tel Aviv 61392, Israel. http://www.tau.ac.il/ramot/danvils.
(36) Barnett, J. D.; Block, S.; Piermarini, G. J. *Rev. Sci. Instum.* **1973**, *44*, 1.
(37) Pines, E.; Huppert, D.; Agmon, N. *J. Chem. Phys.* **1988**, *88*, 5620.
(38) Agmon, N.; Pines, E.; Huppert, D. *J. Chem. Phys.* **1988**, *88*, 5631.
(39) Debye, P. *Trans. Electrochem. Soc.* **1942**, *82*, 265.
(40) Nakahara, M.; Osugi, J. *Rev. Phys. Chem. Jpn.* **1980**, *50*, 66.
(41) Bridgman, P. E. *The Physics of High Pressure*; G. Bell and sons Ltd.: London, 1958.
(42) Andrussow, L.; Schramm, B., Landolt-Bornstein, Schaffer, K., Eds.; Springer: Berlin, 1969; Vol. 2, Part 5a.
(43) Agmon, N.; Goldberg, S. Y.; Huppert, D. *J. Mol. Liquids* **1995**, *64*, 161.
(44) Lee, J.; Robinson, G. W.; Bassez, M. P. *J. Am. Chem. Soc.* **1986**, *37*, 127.
(45) Kreevoy, M. M.; Kotchevar, A. T. *J. Am. Chem. Soc.* **1990**, *112*, 3579. Kotchevar, A. T.; Kreevoy, M. M. *J. Phys. Chem.* **1991**, *95*, 10345.
(46) Rips, I.; Jortner, J. *J. Chem. Phys.* **1987**, *87*, 2090.
(47) Agmon, N.; Levine, R. D. *Chem. Phys. Lett.* **1977**, *52*, 197. Agmon, N.; Levine, R. D. *Israel J. Chem.* **1980**, *19*, 330.
(48) Bromberg, S.; Chan, I.; Schilke, D.; Stehlik, D. *J. Chem. Phys.* **1993**, *98*, 6284.
(49) Pottel, R.; Asselborn, E. *Ber. Bunsen-Ges. Phys. Chem.* **1980**, *84*, 462.
(50) Pines, E.; Fleming, G. R. *Chem. Phys. Lett.* **1994**, *183*, 393.
(51) Pines, E.; Magnes, B.; Lang, M. J.; Fleming, G. R. *Chem. Phys. Lett.* **1997**, *281*, 413.
(52) Solntsev, K.; Huppert, D.; Agmon, N. *J. Phys. Chem. A* **2000**, *104*, 4658.
(53) Johari, G.; Dannhauser, W. *J. Chem. Phys.* **1969**, *50*, 1862.
(54) Johari, G.; Dannhauser, W. *J. Chem. Phys.* **1969**, *51*, 1626.
(55) Hilbert, R.; Todheide, K.; Franck, E. U. *Ber. Bunsen-Ges. Phys. Chem.* **1981**, *85*, 636.